LA-3752

LOS ALAMOS SCIENTIFIC LABORATORY
of the
University of California
LOS ALAMOS • NEW MEXICO

A 90° ^{3}He Neutron Spectrometer

UNITED STATES
ATOMIC ENERGY COMMISSION
CONTRACT W-7405-ENG. 36

DISCLAIMER

This report expresses the opinions of the author or authors and does not necessarily reflect the opinions or views of the Los Alamos Scientific Laboratory.

Printed in the United States of America. Available from Clearinghouse for Federal Scientific and Technical Information National Bureau of Standards, U. S. Department of Commerce Springfield, Virginia 22151

Price: Printed Copy $3.00; Microfiche $0.65

LA-3752
UC-34, PHYSICS
TID-4500

LOS ALAMOS SCIENTIFIC LABORATORY
of the
University of California
LOS ALAMOS • NEW MEXICO

Report written: September 20, 1967
Report distributed: November 2, 1967

A 90° ^{3}He Neutron Spectrometer

by

W. K. Brown
A. N. Ellis
D. D. Peterson

THIS PAGE

WAS INTENTIONALLY

LEFT BLANK

CONTENTS

THIS PAGE

WAS INTENTIONALLY

LEFT BLANK

A 90° ^{3}He NEUTRON SPECTROMETER

by

W. K. Brown, A. N. Ellis, and D. D. Peterson

ABSTRACT

A fast ^{3}He neutron spectrometer has been developed that is free of recoil spectrum effects. Positioning solid-state detectors outside the neutron beam at 90° yields this advantage, and precludes nuclear reactions in the detectors themselves. Operating in conjunction with a pulse-height analyzer, the spectrometer covers the energy range $0.1 < E_n < 6$ MeV, or higher, with an energy resolution of ~ ±10%. In a time-of-flight, current signal operating mode, the energy range is extended to very low neutron energies. The spectrometer was used in the latter manner to measure the neutron spectrum of the Persimmon experiment conducted at the Nevada Test Site in February 1967.

1. INTRODUCTION

For the Los Alamos time-of-flight neutron cross-section measurements using an underground nuclear explosion source, it is important to have a neutron spectrometer capable of accurately measuring the spectrum over a wide energy range. The spectrometer described in this report was conceived to improve upon the ^{6}Li(n,α)T and ^{235}U(n,f) spectrometers in use.[1] The spectrum from the explosion source, with an intervening moderator, extends from ~ 10 eV to several MeV. The ^{6}Li(n,α)T spectrometer is limited to energies below ~ 10 keV due to uncertainties in the ^{6}Li cross section above this point. The ^{235}U (n,f) spectrometer covers the energy range above ~ 1 keV; the limit arising because of increasingly large fluctuations in the cross section below this energy.

The search for a better spectrometer led to one based on the ^{3}He(n,p)T reaction. This reaction offers several advantages: It could be seen that there was promise of covering the entire energy range with a ^{3}He spectrometer. The reaction energy is high enough to provide a healthy signal-to-noise ratio; and the smooth, slowly varying cross section is well known. The fact that ^{3}He is an inert gas ensures uniformity of the material in the beam and permits the atomic density to be determined accurately by a simple pressure-temperature measurement.

A disadvantage of ^{3}He spectrometers is the presence of the ^{3}He recoil spectrum from the elastic scattering reaction. Although two methods have been devised to eliminate this bothersome factor,[2-5] both have drawbacks. If the spectrometer could be designed so that its response was dependent only on particles emitted at an angle of 90° (or more) to the neutron beam direction, then recoiling ^{3}He nuclei would have no effect. Such a system, sensitive only to particles in a limited solid angle at 90°, would necessarily have its efficiency reduced by a factor of, perhaps, 100; but this would be acceptable because of the high

intensity of the neutron beam from the nuclear explosion. The biggest unknown in the performance of such a spectrometer was its response to the background present in the experiment. Not much is known about this background; but, typically, it is high following the gamma flash from the source, decays with a time constant of 5 to 6 μsec, and is negligibly small below ~ 10 keV neutron energy. Therefore, it was not known if the foreground-to-background ratio would be large enough at high energies, nor was it known if the background could be adequately measured.

2. PRINCIPLES

The spectrometer was conceived as a flat cylindrical volume through which the beam would pass, on-axis, through thin windows. Small solid-state detectors, connected in parallel, would ring the periphery of the cylinder inside the gas envelope at 90°. In the energy range of interest, three reactions take place in ^{3}He:

^{3}He(n,p)T	Q_{np} = +0.764 MeV
^{3}He(n,n)^{3}He$^+$	
^{3}He(n,d)D	Q_{nd} = -3.27 MeV
	(E_{th} = 4.36 MeV)

In addition, at higher energies two other reactions are known:

^{3}He(n; p,n)D	E_{th} ~ 7.3 MeV
^{3}He(n; p,2n)^{1}H	E_{th} ~ 10.3 MeV

It was felt that the two higher-energy reactions would not interfere, but certainly the (n,d) reaction and the contribution of the protons and tritons from the (n,p) reaction should be investigated.

In the laboratory system, the various particle energies are:

$$E_{pL} = \frac{E_n}{16}\left[\mu_L + \left(8 + \frac{12Q_{np}}{E_n} + \mu_L^2\right)^{1/2}\right]^2 \qquad (1)$$

$$\mu_L \equiv \cos \varphi_L$$

$$E_{TL} = \frac{3E_n}{16}\left[\mu_L + \left(\frac{4Q_{np}}{3E_n} + \mu_L^2\right)^{1/2}\right]^2 \qquad (2)$$

$$E_{^3HeL} = \frac{3E_n}{4}\mu_L^2 \qquad (3)$$

$$E_{DL} = \frac{E_n}{8}\left[\mu_L + \left(2 + \frac{4Q_{nd}}{E_n} + \mu_L^2\right)^{1/2}\right]^2 \qquad (4)$$

where φ_L is the laboratory emission angle of the particular particle in each case.

Limiting the spectrometer response to particles emitted at $\varphi_L = 90°$ yields:

$$E_{pL}(90°) = \frac{E_n}{2} + \frac{3}{4}Q_{np} \qquad (5)$$

$$\left(\tfrac{3}{4}Q_{n,p} = 0.573 \text{ MeV}\right)$$

$$E_{TL}(90°) = \frac{Q_{np}}{4} \qquad (6)$$

$$\left(\tfrac{1}{4}Q_{n,p} = 0.191 \text{ MeV}\right)$$

$$E_{^3HeL}(90°) = 0 \qquad (7)$$

$$E_{DL}(90°) = \frac{E_n}{4} + \frac{Q_{nd}}{2}\,. \qquad (8)$$

Two facts are immediately apparent: First, deuterons from the (n,d) reaction cannot reach a detector at 90° unless the initiating neutron has an energy $E_n \geq 2Q_{nd}$ or 6.54 MeV. Thus, the range is extended upward to this energy without any complication. Second, tritons from the (n,p) reaction emitted at 90° have an energy of $Q_{np}/4$ regardless of the initiating neutron energy. This advantageous situation is discussed in Section 7. Briefly, as it is desirable to maximize ^{3}He pressure to attain high efficiency, tritons will inevitably lose a large fraction of their initial energy in the gas as well as in the detector windows. It is convenient to adjust the ^{3}He pressure so that tritons are stopped completely, resulting in an unambiguous and simple dependence of the spectrometer response on protons alone.

In any case, the ^{3}He pressure limit is reached when an appreciable part of the proton energy is lost in the gas. This criterion limits the ^{3}He pressure to a few tenths of an atmosphere--down roughly a factor of ten from typical high-pressure ^{3}He proportional counters now available.

The result of this design is a fast-response spectrometer having a spectrum uncomplicated by competing reactions up to 6 MeV. The price paid for these features is a reduction in efficiency of

about 10^3 with respect to other ^{3}He spectrometers. The reduction is a combined effect of limited solid angle of particle acceptance and limited ^{3}He pressure. However, in our particular application of the spectrometer to explosion source beams, the reduced efficiency of the 90° design is not a disadvantage because of the high neutron intensity.

3. COUNTER DESIGN

The criteria for counter design are as follows:

1. The reaction-site-volume/detector combination must subtend as small an angle as possible to limit both the energy spread of the protons reaching the detectors and the maximum triton energy that must be stopped. A collimator must be interposed between the beam and the detectors to define the angle.

2. The ^{3}He pressure must be as high as possible for high efficiency. The limit is reached at the point where protons lose an appreciable fraction of their energy before striking the solid-state detectors.

3. Detectors are placed in a circle around the beam to detect a larger fraction of the protons emitted at 90° and to make the spectrometer insensitive to off-center passage of the neutron beam. The detectors must be located outside the beam at a distance well away from its fringes to avoid nuclear reactions in the detectors themselves.

4. The solid-state detectors must have a sensitive layer thick enough to stop protons of the highest expected energy. The detector windows must be thin enough that they will not remove an excessive amount of energy from the protons.

5. The spectrometer windows must be as thin as possible to minimize interference with the beam, yet strong enough to hold 1 atm inward pressure (during pumpout prior to filling). The windows must be large enough to accept the entire neutron beam, but no larger than necessary. To eliminate background contributions from the windows, they must be hidden from the detectors.

Using these criteria, we designed a spectrometer to measure the neutron energy spectrum in the beam of the Persimmon experiment of February 1967. Figure 1 shows the spectrometer in cross section, with pertinent dimensions. Figure 2 shows the plastic support holding the ring of solid-state detectors, brass body, nickel windows, proton collimator, and other spectrometer components. Figure 3 shows the assembled ^{3}He spectrometer mounted above an identical spectrometer filled with ^{4}He for an attempted simultaneous background measurement.

The detectors chosen for this application are silicon p-n type, diffused-junction, 200 ohm-cm detectors. The detectors have a nominal 1 cm x 1 cm square sensitive area, and a sensitive layer depth of about 60 μ when operated at a bias of 180 V (near maximum for this detector). The silicon windows through which the protons and tritons must pass are 0.9 ± 0.1 μ thick. The sensitive layer depth of 60 μ is sufficient to stop ~ 2.4-MeV protons; i.e., 90° protons initiated by ~ 3.6-MeV neutrons. Thicker detectors would, of course, provide a higher neutron energy limit.

4. PULSE MODE OPERATION

With the output directed to a pulse-height analyzer, this spectrometer operates much as do other ^{3}He solid-state neutron spectrometers.[6] As mentioned previously, the elimination of the ^{3}He recoil spectrum has been obtained at the cost of reduced efficiency.

Characteristics

The energy range is limited at the lower end to about 0.1 MeV by the fact that the reaction energy is 0.764 MeV. If we assume that the effects of the (n,d) reaction above 6.54 MeV could be unfolded, the upper limit could be extended to perhaps 14 MeV for continuous spectra, depending on how much and at what point the (n;p,n) and (n;p,2n) reactions interfere. A recent publication shows that such spectrometers can be used for discrete energy spectra to energies as high as 20 MeV.[7]

The pulse-height scale is proportional to the proton energy at 90°, Eq. (5), minus the proton energy loss in the gas and windows. These losses can be calculated rather easily and pose no great problem.

The resolution is dominated by the spread in proton energy arising from the finite angle subtended by the detector about 90°. Differentiating Eq. (1) with respect to μ_L and subsequently introducing the approximation that $\mu_L \approx 0$ yields

$$\Delta E_{pL} \approx \frac{E_n}{8}\sqrt{8 + \frac{12Q_{np}}{E_n}}\cdot\Delta\mu_L = \frac{1}{2}\sqrt{E_n E_{pL}(90^\circ)}\cdot\Delta\mu_L. \quad (9)$$

The resolution is given by the ratio of this energy (pulse-height) spread to the energy scale above the zero neutron energy point at $3Q_{np}/4$. As this scale is proportional to $E_n/2$ (neglecting the loss in the gas and windows), the resolution in neutron energy is approximately

$$\frac{\Delta E_{pL}}{E_n/2} \approx \frac{1}{4}\sqrt{8 + \frac{12Q_{np}}{E_n}} \cdot \Delta\mu_L = \sqrt{\frac{E_{pL}(90^\circ)}{E_n}} \cdot \Delta\mu_L . \qquad (10)$$

A quick calculation shows that the resolution can be held to a reasonable value only if $\Delta\mu_L \leq \pm 0.1$, i.e., $\omega_L \approx 90 \pm 6$ degrees.

The efficiency of the spectrometer depends on several factors, including the atomic density, the nuclear cross section, and the fraction of solid angle subtended by the detectors. The efficiency is also dependent on the relative angular proton emission probability at 90° in the laboratory system,

$$g_{pL}(E_n) \equiv \frac{\frac{d\sigma_{np}}{d\Omega_L}(E_n, 90^\circ)}{\sigma_{np}(E_n)/4\pi} . \qquad (11)$$

This quantity will be investigated in Section 7.

Applications

Aside from ordinary neutron spectrometry applications, this 90° design may also find use as a flux monitor--as a transmission detector in thermal neutron reactor beams, for example. Its main advantage over present monitors[8] for such purposes is the response time--a few nanoseconds in this design vs several microseconds in the case of a proportional counter. The absolute precision of the 90° design used as a flux monitor may be limited to 1 to 2% by uncertainties in measurement of the subtended solid angle of the detectors. The absolute efficiency could be determined to < 1% by simultaneous measurement in a thermal neutron beam vs a precision ^{3}He proportional counter,[8] or gold foil activation.[9] If the instrument is used as a beam monitor, a discriminator setting corresponding to about 400 keV eliminates essentially all the electronic, (n,γ), and other background pulses without loss of legitimate $^3\mathrm{He}(n,p)\mathrm{T}$ events.

Application may also be found in neutron time-of-flight work at higher energies--up to ~ 6 MeV for continuous spectra, and perhaps as high as 20 MeV for discrete spectra--as mentioned previously. As a transmission beam monitor, its main competitor would perhaps be the ^{3}He scintillation detector, although such a detector requires maintenance of a very high gas purity whereas the 90° solid-state design does not. The stability of photomultiplier tubes vs solid-state detectors is also a factor.

Although in most cases the highest possible efficiency is desirable, if in any particular application a lower count rate is required, this can be easily achieved. The count rate could be lowered by decreasing the ^{3}He pressure (thicker detector windows would stop the tritons), reducing the proton collimator aperture, or reducing the size or number of the detectors. In the simplest case, a single detector placed to one side of the beam constitutes a spectrometer or beam monitor. However, if the ring geometry is forsaken, the detection efficiency is no longer independent of the beam position.

The above discussion concerns the pertinent attributes of the spectrometer operated in the normal pulse mode. The application for which the spectrometer was designed and used was the extremely high reaction rate regime of nuclear explosion source beam measurements; i.e., the current mode. As the spectrometer was used only in the current mode, the remaining discussion emphasizes this application. Nevertheless, much of the material is relevant to both modes of operation.

5. CURRENT MODE OPERATION

Operation in the current mode is characterized by the detection of a large number of events per resolving time. The resulting current comprises a time-varying analog signal. In neutron time-of-flight cross-section measurements in which time is uniquely related to neutron energy, the analog signal, at any particular time, is proportional to the neutron flux and the neutron cross section of the target material at the corresponding energy. From a time recording of this signal, the neutron spectrum is obtained directly.

Note that all pulse-height information is sacrificed in obtaining a sufficient number of detected events per resolving time to give good statistics. The energy scale is thus defined by the time of flight alone. The energy range, now having no lower limit, is $0 < E_n < 6.5$ MeV. (The upper limit was

discussed previously.) The energy resolution of the spectrometer is now dependent on the time resolution of the system--the detectors, the amplifier, and the recording system. The resolution is no longer dependent on the angular (energy) spread of the detected protons, because the current signal is proportional to the average energy of the protons striking the detectors within the resolving time.

The concept of efficiency is the same as in the pulse mode case, as the efficiency is dependent on atomic density, nuclear cross section, relative probability of 90° proton emission, and geometrical solid angle. The interpretation of the response in the current mode is simplified by the absence of the ^{3}He recoil spectrum, as before.

6. TIME OF FLIGHT -- CURRENT SIGNAL PRINCIPLES

For neutrons, the relation among energy, flight path, and time of flight is given by

$$E_n = 5227 \frac{\ell^2}{t^2} \tag{12}$$

where the units are E (eV), ℓ (meters), and t (μsec). Typical flight paths used in our explosion source cross-section measurements are 200 to 300 meters. By placing a moderator above the explosion source, an energy spectrum between 10 eV and several MeV is obtained. Fission neutrons, therefore, arrive at the targets after 10 to 20 μsec; and the last neutrons arrive in, typically, 5 msec--thus defining the required recording time span.

Differentiation of Eq. (12) yields the energy resolution in terms of the time resolution:

$$\frac{dE_n}{dt} = -10454 \frac{\ell^2}{t^3} = -0.02766 \frac{E_n^{3/2}}{\ell} . \tag{13}$$

The time resolution of the source is dependent on the burst time of $\sim$ 0.1 μsec, the physical size of the source, and (at lower energies) the holdup time of the moderator. The rather complicated result of these combined effects has been discussed elsewhere;[1] but, in any case, all other system components are designed to match the shortest time associated with the source; i.e., 0.1 μsec.

To achieve adequate statistical accuracy (3%) in the analog signal, it is therefore necessary to plan the experimental conditions to obtain a detected event rate of 1000 counts per 0.1 μsec. The first step in planning for such a level is advance knowledge of the approximate neutron spectrum. Calculations from both theory and experimental results are fruitful.

Spectra

First, it is possible to estimate the spectrum shape by knowing the fission spectrum, the fact that the source is surrounded by hot hydrogenous material (high explosive) at the time of neutron emission,[10] and the typical 1/E plus Maxwellian distribution of the polyethylene moderator. The estimated shape can be normalized to the total number of neutrons produced, S, which, in turn, can be determined from the expected energy yield, Y (kilotons), of the explosive:

$$Y \propto S = \int_0^\infty S(E_n) dE_n . \tag{14}$$

At the end of the flight path, the estimated spectrum is the fraction directed toward the ground surface in the solid angle Ω_ℓ defined by the collimator orifice of area A_o at distance ℓ:

$$n(E_n) = \frac{\Omega_\ell}{4\pi} S(E_n) = \frac{A_o}{4\pi\ell^2} S(E_n). \tag{15}$$

The quantity required is the total neutron current (in neutrons per unit time passing through the collimator orifice), which is related to the above energy spectrum by

$$n(t)dt = n(E_n)dE_n . \tag{16}$$

Note that the "flux," in neutrons/cm^{2}sec, is equal to $n(t)/A_o$. On the other hand, perhaps more confidence results from studying neutron spectra observed in past experiments. In this connection it is germane to note that the quantity n(t) does not change appreciably from experiment to experiment, because the safe burial depth, ℓ, (the flight path) is dictated by the energy yield, Y, by the empirical formula

$$\ell = 122\, Y^{1/3} . \tag{17}$$

By combining Eq. (13) through (17) the constancy of n(t) is demonstrated:

$$n(t) = n(E_n) \frac{dE_n}{dt} \propto \Omega_\ell \cdot Y \cdot \frac{dE_n}{dt}$$

$$\propto \frac{1}{\ell^2} \cdot \ell^3 \cdot \frac{1}{\ell} = \text{constant}. \tag{18}$$

Figure 4 shows the spectra observed in the previous two experiments: Parrot (December 1964, no moderator) and Petrel (June 1965, with moderator). Note that the ordinate is $E_n \cdot n(E_n)$, in units of neutrons per natural logarithmic energy decrement, per cm^2. (Division of the ordinate by $\ell n\ 10 = 2.301$ would yield units of neutrons per decade per cm^2). These units are identical to nuclear reactor physicists' "lethargy" units and are useful for two reasons: They allow convenient plotting of the spectra, and they show the 1/E spectrum as a constant value, a fact of special significance, as will be seen.

Optimum Spectrum

It is clear that the dynamic range of the analog signal from, for example, a fission target will be large. The variation of such a cross section alone is, typically, 10^3 in the resonance region, and this is in addition to the variation in the average of $n(t)\sigma(E_n)$. Only the latter quantity may be controlled (by tailoring the spectrum properly), and it is obviously desirable to hold it constant. If the cross section has a 1/v dependence and the spectrum has a 1/E shape, the combination results in a constant detected event rate, D(t):

$$D(t) \propto n(t)\ \sigma(E_n) = n(E_n)\ \frac{dE_n}{dt}\ \sigma(E_n)$$

$$\propto \frac{1}{E_n} \cdot E_n^{3/2} \cdot \frac{1}{v} = \text{constant}, \qquad (19)$$

and the desired result is achieved. Thus, in this ideal case, a constant $E_n \cdot n(E_n)$ generates a constant detected event rate in a 1/v detector. Note that if the cross section were constant, D(t) would be proportional to n(t) and that the ideal spectrum would be n(t) = constant.

A useful relationship between the energy and time spectra is

$$2E_n \cdot n(E_n) = t \cdot n(t). \qquad (20)$$

7. CURRENT MODE ANALYSIS

The reaction rate, R(t), in the target is related to the neutron flux, the atomic surface density, and the nuclear cross section by

$$R(t) = n(t)\rho_s\sigma_{np}(E_n) = n(t)\rho_v\bar{T}\sigma_{np}(E_n) \qquad (21)$$

where, for the ^3He spectrometer, the atomic volume density is the measured quantity and $\bar{T}$ is the average target thickness, as seen by the detectors.

The detected event rate is given by

$$D(t) = R(t)g_{pL}(E_n)\Omega_D/4\pi \qquad (22)$$

where $g_{pL}(E_n)$ represents the relative probability of proton emission at 90° in the laboratory system, and $\Omega_D/4\pi$ is the fractional geometrical solid angle subtended by the reaction volume/detector combination.

Finally, the voltage signal, V(t), is given by the detector current, at time t, flowing across the termination resistor, R_{term}.

$$V(t) = \frac{D(t)E_{Dep}(E_n)}{W}\ R_{term} \qquad (23)$$

where $E_{Dep}(E_n)$ is the energy deposited per proton, and W is the energy required to make an ion pair in the detector. Several of the individual quantities must be examined in further detail.

Target Dimensions

The average thickness of the gas target was determined by numerically calculating the effective volume, defined as

$$V_{eff} \equiv \sum \omega_i \Delta_i V \qquad (24)$$

where the weighting factor ω_i for the i^{th} volume element includes the solid angle subtended and the detector aspect (the effective area seen from off-perpendicular). The masking of portions of some detectors by the collimator lips (at positions toward the windows) was included in the solid angle subtended at each point. Dividing this volume by the beam area (over which $\Delta_i V$ was varied) yields the average thickness

$$\bar{T} = \frac{V_{eff}}{A_{beam}}\ . \qquad (25)$$

Substituting

$$\Delta_i V = \Delta_j A \Delta_k Z \qquad (26)$$

in Eq. (24) and summing first over $\Delta_j A$ in each $\Delta_k Z$ yields the sensitivity profile between windows.

Cross Section

The $^3He(n,p)T$ cross section has received the attention of many experimenters whose data have been collected and analyzed in two recent evalua-

tions.[11, 12] A curve of the values used in this application is shown in Fig. 5. Recent measurements indicate that the cross section is 1/v up to $E_n \approx 1$ keV.[13]

Emission Probability

The relative angular proton emission probability $g_{pL}(E_n)$ is extracted from experimentally measured angular distributions. As data are generally given in the center-of-mass (C) system, the kinematic shift $K(E_n)$ must be used to transfer from the laboratory (L) system to the C system.

$$\left(\frac{d\sigma}{d\Omega}\right)_L = K(E_n)\left(\frac{d\sigma}{d\Omega}\right)_C . \tag{27}$$

The relationship is derived from

$$\left(\frac{d\sigma}{d\Omega}\right)_L d\Omega_L = \left(\frac{d\sigma}{d\Omega}\right)_C d\Omega_C . \tag{28}$$

The elemental solid angle in this cylindrically symmetrical geometry is given by

$$d\Omega = 2\pi \sin\varphi \, d\varphi = -2\pi d\mu . \tag{29}$$

Then

$$\left(\frac{d\sigma}{d\Omega}\right)_L = \left(\frac{d\sigma}{d\Omega}\right)_C \frac{d\mu_C}{d\mu_L} \tag{30}$$

so that

$$K(E_n) = \frac{d\mu_C}{d\mu_L} . \tag{31}$$

The L and C proton emission angles are related by

$$\mu_L = \frac{x_p + \mu_C}{\left(1 + x_p^2 + 2x_p\mu_C\right)^{1/2}} . \tag{32}$$

Then

$$K(E_n) = \frac{\mu_L\left(1 + x_p^2 + 2x_p\mu_C\right)}{\left(1 - \mu_L^2\right)x_p + \mu_C} \tag{33}$$

where

$$x_p \equiv \frac{v_C}{v_{pC}} = \frac{1}{\sqrt{3}}\left(\frac{E_n}{3E_n + 4Q_{np}}\right)^{1/2} \tag{34}$$

is the ratio of center-of-mass velocity to the proton velocity in the C system.

At $\varphi_L = 90^\circ$, Eq. (33) becomes

$$\frac{d\mu_C}{d\mu_L} = \sqrt{1 - x_p^2} = \frac{2}{\sqrt{3}}\left(\frac{2E_n + 3Q_{np}}{3E_n + 4Q_{np}}\right)^{1/2} \equiv K_p(E_n) \tag{35}$$

where $K_p(E_n)$ denotes the shift specifically at $\varphi_L = 90^\circ$ for protons. Note that this shift is never very large:

$$1 \geq K_p(E_n) \geq \frac{2\sqrt{2}}{3} = 0.943 \text{ for } 0 \leq E_n \leq \infty . \tag{36}$$

A useful approximation, accurate to better than 0.1%, is that the reduction due to this C-to-L shift of the proton distribution is

$$1 - K_p(E_n) = 1 - \sqrt{1 - x_p^2} \approx \frac{1}{2} x_p^2$$

$$= \frac{1}{6}\left(\frac{E_n}{3E_n + 4Q_{np}}\right). \tag{37}$$

Angular Distribution

The proton angular distribution has been derived primarily from the cross sections observed in the inverse reaction[14-17] by detailed balance. Curves fitted to the collected data are shown in Fig. 6. Coefficients of the cosine series fitted to the data of Perry et al.[14] and Goldberg et al.[15] are shown in Fig. 7.

The cross-section value needed for the present application is that at the value of μ_C for which $\mu_L = 0$. From Eq. (32) it is seen that this condition is satisfied by

$$\mu_C = -x_p = \frac{-1}{\sqrt{3}}\left(\frac{E_n}{3E_n + 4Q_{np}}\right)^{1/2} \quad (\text{for } \mu_L = 0). \tag{38}$$

At each neutron energy, the angular cross section was obtained at this specific angle, and the relative probability of proton emission was evaluated in the C system:

$$g_{pC}(E_n) \equiv \frac{\frac{d\sigma_{np}}{d\Omega_C}(E_n, \varphi_L = 90^\circ)}{\sigma_{np}(E_n)/4\pi} . \tag{39}$$

The denominator is just what the angular cross section would be if the distribution were isotropic. The value of $\sigma_{np}(E_n)$ used here is the integral of the angular distribution and is not necessarily that shown in Fig. 5. In this way, the value of $g_{pC}(E_n)$ is seen to be independent of the cross-section value, and dependent only on the shape of the angular distribution. The values[14-17] are shown in Fig. 8. Values at energies lower than the lowest energy of experimental data were obtained by extrapolating the coefficients shown in Fig. 7 back

to zero energy and then constructing the angular distribution curves therefrom. Values of $\sigma_{np}(E_n)$, $g_{pc}(E_n)$, and uncertainties are listed in Table I, and the spectrometer "response," i.e., $K_p(E_n)g_{pc}(E_n)\sigma_{np}(E_n)$, is shown in Fig. 5.

Table I. $\sigma_{np}(E_n)$ and $g_{pc}(E_n)$ vs E_n

E_n	$\sigma_{np}(E_n)$ (barns)	$g_{pc}(E_n)$	E_n	$\sigma_{np}(E_n)$ (barns)	$g_{pc}(E_n)$
0.0253	5327 ± 10 (1/v)	1	100 keV	1.95 ± 0.1	0.992
100 eV	84.75 ± 0.2	1	150	1.50 ± 0.1	0.987
150	68.9 ± 0.3	1	200	1.28 ± 0.1	0.982
200	59.7 ± 0.3	1	250	1.13 ± 0.1	0.978
250	53.3 ± 0.3	1	300	1.05 ± 0.1	0.973
300	48.7 ± 0.3	1	350	0.98 ± 0.1	0.969
400	42.1 ± 0.3	1	400	0.93 ± 0.09	0.965
500	37.5 ± 0.3	1	450	0.89 ± 0.09	0.961
700	31.7 ± 0.3	1	500	0.87 ± 0.09	0.957
1.0 keV	26.5 ± 0.3	1	600	0.84 ± 0.08	0.948
1.5	21.6 ± 0.3	1	700	0.83 ± 0.08	0.936
2.0	18.6 ± 0.3	1	800	0.83 ± 0.08	0.921
2.5	16.6 ± 0.2	1	900	0.83 ± 0.08	0.906
3.0	15.1 ± 0.2	1	1.0 MeV	0.84 ± 0.08	0.890
4.0	12.8 ± 0.2	1	1.2	0.87 ± 0.09	0.860
5.0	11.4 ± 0.2	1	1.5	0.88 ± 0.09	0.813
7.0	9.5 ± 0.2	1	1.7	0.88 ± 0.09	0.787
10.0	7.7 ± 0.2	1	2.0	0.85 ± 0.09	0.751
15.0	6.1 ± 0.1	1	2.2	0.83 ± 0.08	0.731
20.0	5.2 ± 0.1	1	2.5	0.78 ± 0.08	0.706
25.0	4.6 ± 0.1	1	2.7	0.74 ± 0.07	0.690
30.0	4.1 ± 0.1	1	3.0	0.66 ± 0.07	0.669
40.0	3.4 ± 0.1	1.000	4.0	0.47 ± 0.05	0.611
50.0	3.0 ± 0.1	0.999	5.0	0.37 ± 0.04	0.570
70.0	2.4 ± 0.1	0.996	7.0	0.26 ± 0.03	0.550
			10.0	0.18 ± 0.02	0.699

Uncertainty in g_{pc} is estimated to be $< \pm 0.02$.

Energy Loss

The energy deposited per proton, $E_{Dep}(E_n)$, is equal to the proton energy at 90°, Eq. (5), minus the energy lost in the gas and in the detector window. From data quoted by Whaling[18] and by Whaling and Demirlioglu,[19] these losses may be summarized by

$$E_{p1} = \frac{E_n}{2} + \frac{3}{4} Q_{np}; \quad Q_{np} = 0.764 \text{ MeV} \qquad (40)$$

$$E_{p2} = E_{p1} - \Delta E_g; \quad \Delta E_g = \frac{0.0132}{E_{p1}} \left[\ell n \frac{E_{p1}}{2} + 4.68 \right] \qquad (41)$$

$$E_{p3} = E_{p2} - \Delta E_w; \quad \Delta E_w = \frac{0.0159}{E_{p2}} \left[\ell n \frac{E_{p2}}{14} + 5.1 \right]. \qquad (42)$$

8. PREDICTION OF SIGNAL LEVELS

The preceding information was used to predict the signal level prior to the Persimmon experiment. This is a critical part of the planning, because recording equipment sensitivities must be correctly set before the experiment. First, we examine the case for neutron energies of $E_n < \sim 1$ keV, where the (n,p) cross section is essentially 1/v. For convenience, an ideal spectrum of $E_n \cdot n(E_n) = 1 \times 10^{12}$ through the 3-cm^2 collimator orifice was used (refer to Fig. 4). Equations (21) and (22) are combined to find the detected event rate:

$$D(t) = n(t)\rho_v \bar{T}\sigma_{np}(E_n)K_p(E_n)g_{pc}(E_n)\Omega_D/4\pi. \qquad (43)$$

The ^{3}He density was limited to ~ 1/5 atm for the 2-in. detector spacing chosen (refer to Fig. 1). At this pressure, the protons, emitted at 0.573 MeV ($E_n < 1$ keV) would lose approximately 79 keV in the gas, and 57 keV in the 0.9-μ-thick silicon detector windows. Uncertainties in these losses are about ± 10% due to the ^{3}He stopping cross sections

(= ± 8 keV), ± 10% in window thickness (= ± 6 keV), and ± 10% in silicon stopping cross sections (= ± 6 keV). The combined uncertainty is, thus, approximately ± 11.3 keV or ~ ± 2.6% in proton energy. The proposed atomic density of the ^{3}He was, therefore, 5.38×10^{18} atoms/cm^3. The average target thickness was estimated to be 1.7 cm, and the (n,p) cross section[20] used was

$$\sigma_{np}(E_n) = 5327 \sqrt{\frac{0.0253}{E_n}} = 5327 \sqrt{\frac{0.0253}{5227}} \frac{t}{\ell}. \quad (44)$$

The flight path was to be about 300 m. It was planned to use a ring of eight, evenly spaced, 1 cm^2, solid-state detectors. At a spacing of 2 in. these would subtend a solid angle of 2.47% of 4π steradians. The values of both $K_p(E_n)$ and $g_{pc}(E_n)$ are close to unity for $E_n < 1$ keV, so that, for neutron energies less than 1 keV, the ideal situation described in Section 6 prevails; and the detected event rate is constant. When the above numerical values are substituted in Eq. (43), the predicted detected event rate becomes

$$D(t) = 3 \times 10^{10} \text{ counts per sec.}$$

In the resolving time of 0.1 μsec, therefore, about 3000 counts will be registered, and uncertainties in counting statistics will be less than 2%.

The expected signal level may now be calculated from Eq. (23). The energy loss for a proton at low neutron energies and at 1/5-atm ^{3}He pressure is 79 keV in the gas and 57 keV in the detector windows. Having been emitted with an initial energy of 0.573 MeV, the protons deposit an energy of 0.437 MeV. The energy required to make an ion pair, W, is taken as 3.58 eV,[21] and the detector current is therefore 0.6 mA. (The detectors can carry quite large currents with no complication.)[22] Across a 50-Ω terminator, this current would comprise a voltage of 30 mV, sufficiently high to provide an adequate signal-to-noise ratio, as the amplifier noise and baseline uncertainty is typically 0.1 mV.

Table II shows a prediction of the signal level for $E_n \geq 1$ keV, again for a spectrum of $E_n \cdot n(E_n) = 1 \times 10^{12}$.

Note that in Eq. (43), if $g_{pc}(E_n)$ is written explicitly, the cross section cancels out and

$$D(t) = n(t)\rho_v \bar{T} K_p(E_n) \frac{d\sigma_{np}}{d\Omega_c}(E_n, \varphi_L = 90^\circ)\Omega_D. \quad (45)$$

This is simply an alternative way of writing Eq. (43). Equation (43) seems preferable as it retains the evaluated $\sigma_{np}(E_n)$ and shape-only dependent $g_{pc}(E_n)$.

Table II. Predicted Signal Levels

E_n	$\sigma_{np}(E_n)$ (barns)	$K_p(E_n)$	$g_{pc}(E_n)$	ΔE_g (MeV)	ΔE_w (MeV)	$E_{Dep}(E_n)$ (MeV)	Signal (mV)	Time (μsec)
1 keV	26.5	1.000	1.000	0.079	0.057	0.437	30	702
10	7.7	0.999	1.000	0.079	0.057	0.442	28	222
100	1.95	0.995	0.992	0.074	0.054	0.495	24	70.2
1 MeV	0.84	0.972	0.900	0.050	0.039	0.984	59	22.2
2	0.85	0.964	0.750	0.037	0.030	1.506	106	15.7
3	0.66	0.959	0.667	0.030	0.025	2.018	120	12.8
4	0.47	0.955	0.606	0.025	0.021	2.527	111	11.1

9. CORRECTIONS AND UNCERTAINTIES

It has been shown that the uncertainty in proton energy loss is ~ ±2.6%, and that the counting statistics give ~ ±2%. It is not difficult to measure the ^{3}He pressure with better than 1% precision. The average counter thickness, determined numerically (Section 7), was found to be 1.76 cm. Figure 9 shows the sensitivity of the reaction volume/detector combination. It was subsequently noted that lines drawn from the center of a detector through the edges of the upper and lower collimator lips defined a length on the center line equal to 1.77 cm. The uncertainty in $\bar{T}$ has been estimated to be 0.01 cm.

Detector areas were measured in two ways: by determining the count rate at a known distance from a calibrated ^{239}Pu alpha source, and physically, by using a comparator. The measurement of the seven detectors available for the ^{3}He spectrometer in the Persimmon experiment with the alpha source provided 1 to 2% precision, while the direct visual measurement had an estimated uncertainty of 3.7%. Total areas of the seven detectors from the two methods differed by 2.7%; and, therefore, the results were in agreement. The total area was determined to be 5.01 ± 0.08 cm^2, which at a distance of 2 in. subtends a solid angle of 1.55% of 4π steradians. Note that although the detectors were purported to be "1 cm^2" detectors, the areas actually averaged ~ 5/7 cm^2.

Geometrical Solid Angle

The above solid-angle calculation was made on the simplifying assumption that all events occurred at the center of the spectrometer. Actually, the ^{3}He(n,p)T reactions occur over a finite volume defined by the beam diameter and the geometry. As seen from a particular detector, the average reaction site appears to be at a distance slightly closer to the detector; and the calculated correction of 1.5% means that the solid angle should be adjusted to 1.57 ± 0.03% of 4π steradians.

Average Proton Energy

By assuming an isotropic emission from the center, the average of the distribution in proton energy due to the finite angle subtended by the detectors was calculated; the value was found to differ from the 90° figure by $< +0.3\%$ at $E_n = 4$ MeV. (The plus sign denotes an increase in average energy.) The difference decreases with decreasing energy and can be neglected. The converse calculation, i.e., from all points along the spectrometer axis to the center of a counter, gave the same result.

The shifts of the average proton energy due to the changing kinematic shift and angular cross section were calculated in the same manner. The shift at 4 MeV was -0.82%, and it was also neglected because it also is relatively small and decreases with decreasing energy, and (especially) because it is in the opposite direction to the shifts described above.

Outscattering

The outscattering of protons passing through the ^{3}He gas (primarily Coulomb scattering) is negligible. Calculating the worst case, i.e., at E_p = 0.573 MeV, showed that approximately 10^{-4} of the protons scatter out.

Tritons

The effects of tritons must be examined more closely. The stopping cross-section curves are of such a shape that the tritons with energies of interest meet the most efficient stopping. Still, at higher neutron energies tritons emitted in the rear of the spectrometer and at such an angle as to strike the extreme front of the detectors are not completely stopped. (The worst case in the spectrometer described here is $\varphi_L = 72.6°$.) Equation (2) gives the triton energy as a function of neutron energy and angle. Other pertinent equations can be derived:

$$x_T \equiv \frac{v_C}{v_{TC}} = \sqrt{3}\left(\frac{E_n}{3E_n + 4Q_{np}}\right)^{1/2} \quad (= 3x_p), \tag{46}$$

$$K(E_n) = \frac{\mu_L(1 + x_T^2 + 2x_T\mu_C)}{(1 - \mu_L^2)x_T + \mu_C}. \tag{47}$$

At $\varphi_L = 90°$:

$$K_T(E_n) = \sqrt{1 - x_T^2} = \left(\frac{4Q_{np}}{3E_n + 4Q_{np}}\right)^{1/2}, \tag{48}$$

and

$$g_{TC}(E_n) \equiv \frac{\frac{d\sigma_{nT}}{d\Omega_C}(E_n, \varphi_L = 90°)}{\sigma_{np}(E_n)/4\pi} \tag{49}$$

for

$$\mu_C = -x_T. \tag{50}$$

Figure 10 shows the function $g_{TC}(E_n)$. Note that the altered form of $K_T(E_n)$ means that the amount reaching the detectors at 90° decreases for larger neutron energy as the laboratory distribution becomes increasingly weighted in the forward direction. Thus, although the energy deposited per triton grows with increasing energy, the probability of triton emission in the detector direction decreases. Calculations show that the correction rises to a maximum of about +0.2% at E_n = 2 MeV, then decreases again. This effect can, therefore, be neglected.

^{3}He Recoils

Calculation shows that at 1/5-atm He pressure with 2-in. spacing all ^{3}He recoil ions are stopped before they can deposit energy in the sensitive layer of the detectors.

Deuterons

It has been shown in Eq. (8) that it is not kinetically possible for deuterons to be emitted at 90° until $E_n \geq 6.54$ MeV. Of course, at the front edge of the detectors some effect is felt at slightly lower energy, namely at E_n = 6.26 MeV for the worst possible case at $\varphi_L = 72.6°$. Pertinent equations for deuterons include

$$x_D = \frac{v_C}{v_{DC}} = \left(\frac{E_n}{3E_n + 4Q_{nd}}\right)^{1/2} \quad (Q_{nd} = -3.27 \text{ MeV}) \tag{51}$$

$$K(E_n) = \frac{\mu_L(1 + x_D^2 + 2x_D\mu_C)}{(1 - \mu_L^2)x_D + \mu_C} . \tag{52}$$

At 90°

$$K_D(E_n) = \sqrt{1 - x_D^2} = \sqrt{2}\left(\frac{E_n + 2Q_{nd}}{3E_n + 4Q_{nd}}\right)^{1/2} , \tag{53}$$

and

$$g_{DC}(E_n) = 2\frac{\frac{d\sigma_{nd}}{d\Omega_C}(E_n, \varphi_L = 90^\circ)}{\sigma_{np}(E_n)/4\pi} \tag{54}$$

for

$$\mu_C = -x_D , \tag{55}$$

where a factor of two has been included in the last equation to account for the fact that there are two deuterons emitted in each reaction. Note that $K_D(E_n) = 0$ until $E_n \geq 2Q_{nd}$.

Charge Collection

Another possible source of uncertainty is the collection of charge produced by various particles in the He gas. This charge will cause an additional current flow, related in a complicated way to the neutron time spectrum, the various neutron cross sections, the stopping cross sections, and the geometry. The electron drift velocity in 1/5-atm He at 180 V (the detector bias voltage) is approximately 0.4 cm/μsec.[23] The electron transit time from beam center to detector (2 in.) is therefore about 13 μsec--a time that would obviously hurt the resolution if the effect were big enough. The positive ions would be expected to move a few thousand times slower, and probably would not cause much of an effect.

To guess at the magnitude of this problem, note that while 3.58 eV/ion pair is required in the detector, 42.3 eV/ion pair is required in the gas,[24] a factor of 12 increase. On the other hand, the detectors subtend a fractional solid angle of about 2%, so there are some 50 times as many protons alone being produced, aside from all the tritons, ^{3}He ions, and deuterons. In an attempt to avoid the effects of collecting charged particles, the detectors have been connected so that the bias voltage appears on the detector case. While there is no stringent time-resolution requirement (the flux, and (n,p) cross section are smoothly varying), it was necessary to try to measure this effect, so that it might be subtracted. This background measurement is discussed later.

Light Sensitivity

There is also the question of detector light sensitivity. Helium scintillation is a well-known phenomenon and in ^{4}He is characterized by the strongest line of its atomic spectrum at 21.22 eV or 583 Å. Morse et al.[25] have reported the far ultraviolet response (500 to 2000 Å) of silicon p-n junction photodiodes. An attempt was made to measure this background, as described below.

Background Measurement

Backgrounds in the explosion source signals are not well understood. In the case of fission cross-section measurements, the signal from a blank foil is recorded along with the fission signal and later subtracted from it. This procedure has given excellent results, and suggested the use of an identical spectrometer filled with ^{4}He to supply the background signal for the ^{3}He spectrometer. Difference in response between the two spectrometers could only result from differences in the nuclear characteristics of ^{3}He and ^{4}He.

The ^{4}He spectrometer, for example, would duplicate the effects of recoiling ^{3}He ions creating charged particles and causing scintillations. It would not, however, measure these same effects caused by protons, tritons, or deuterons.

Another unknown was the reaction of the spectrometers to the large gamma flux up the vacuum pipe at explosion time. This, in fact, causes the major portion of the observed background. Possible effects arise from the production of Compton electrons in the windows, target foils, etc., but these seem to be unimportant for the ^{3}He spectrometer. Typically, at zero time the background signal for fission measurements rises to several volts (compared to ~ 0.1 V predicted for the ^{3}He spectrometer) and subsequently decays with a time constant of ~ 8 μsec. In fission measurements, at a time corresponding to

an energy of ~ 10 keV, this signal is negligibly small. The decay is not understood, but it can possibly be ascribed to characteristics of the logarithmic amplifiers.

10. THE PERSIMMON EXPERIMENT

Preparations were begun in 1966 to use the ^{3}He spectrometer in the Persimmon experiment. Persimmon featured a vacuum flight path of $\ell \approx 307$ meters, a collimator orifice of ~ 3 cm^2, and an estimated neutron spectrum of $E_n \cdot n(E_n) \approx 1 \times 10^{12}$ as described previously. Three spectrometers were used: ^{6}Li(n,α)T, ^{235}U(n,f), and ^{3}He(n,p)T.

The ^{3}He spectrometer and its ^{4}He background twin were positioned above several other samples at a flight path of 306.87 meters. The assembled spectrometers are shown in Fig. 3. A gas filling system, shown in Fig. 11, and schematically in Fig. 12, was made and tested before the experiment. The spectrometers were filled with their respective gases 1 week before the experiment to pressures (at 44.5°F) as follows:

^{3}He: 150.4 ± 0.2 mm Hg
^{4}He: 150.0 ± 0.2 mm Hg.

The ^{3}He was Mound Laboratory "Normal Grade," and the ^{4}He was Los Alamos "tank" helium (99.9% purity). The spectrometers were recovered, undamaged, about 2 weeks after the experiment. Mass spectroscopic analyses of gas samples taken at the time of filling and after recovery showed that no leakage had occurred. Both spectrometers tested leak-tight after the experiment.

After correction for the small fraction of impurities present (primarily ^{4}He and outgassed O_2 and N_2 in the ^{3}He) the atomic densities in the spectrometers at the time of the experiment were found to be ^{3}He: 5.16×10^{18} ^{3}He atoms/cm^3, and ^{4}He: 5.17×10^{18} ^{4}He atoms/cm^3, with estimated uncertainties of < ± 0.5%. The Persimmon experiment was conducted on February 23, 1967 at the Nevada Test Site.

Data Recording

The analog signals were fed to logarithmic amplifiers[26] (bottom decade linear, plus four log decades above) to reduce the dynamic range in recording. The current signals traveled down an ~ 300-m cable run and formed voltage signals across terminating resistors. The signals were displayed on fast-phosphor oscilloscopes and recorded on moving film[1] with demagnification of 22.3x. Both signals were recorded in a "high" resolution (raster, ~ 0.2 μsec) and a "low" resolution (streak, ~ 1 μsec) mode.[1] A timing signal was recorded alongside the ^{3}He and ^{4}He signals to provide a measurement of the time of flight and to establish a baseline reference. A few hundred milliseconds after the end of the data acquisition, stair-step calibrations were switched into the inputs of the logarithmic amplifiers and recorded on the same film. The films of the ^{3}He and ^{4}He streak recording are shown in Fig. 13.

Data Processing

The signals were digitized with a 30x magnification projection microscope comparator, and the signal level and time coordinates of each point were recorded with an on-line IBM card punch. The digital data were processed through computer codes[27] to perform the operations described in this report. The punched data are first fed through a code to separate the various signals which were read together, and are then transferred to magnetic tape. A second code applies a least-squares adjustment to the base reference and time-mark information to minimize reading errors. Thirdly, codes process the streak or raster data to account for the amplifier characteristics and calibration and, ultimately, yield the signal (in mV) as a function of time, as shown in Fig. 14. To obtain a history of the signal just before the data are recorded, these data are processed by a fourth code, with output as shown in Fig. 15. A fifth and final computer code* is used to transform the data to the form of signal (mV) vs neutron energy and to subtract the ^{4}He background from the ^{3}He foreground and, performing the various operations outlined in Section 7, to yield the neutron spectrum as a function of energy (Fig. 16). Shown also in Fig. 16 is the predicted level for the Persimmon experiment. The dips in the spectrum curve are due to absorption of neutrons in the resonances of samples through which the beam passed before arriving at the ^{3}He spectrometer.

Precision

Aside from the uncertainties and corrections

*The above codes are: (1) SORT, (2) BARFIT, (3) STRK and MVY2, (4) HUM, and (5) SIGER.

discussed in Section 9, the precision of the digitization process must be examined. The accuracy of the comparator is apparently ± 1 μ. The width of the signal lines was 30 μ, and that of the baseline reference was 24 μ. It was found that the center of a single line could be located with an accuracy of ± 1μ, so it is safe to assume that the true line center is being recorded with ~ 2-μ precision. Operator fatigue and inattention may make it more reasonable to adopt an uncertainty of ~ ±10% of the line width.

On the logarithmic scale the uncertainty in signal voltage is related to the line width by

$$\frac{\Delta V_i}{V_i} = \frac{\ell n 10}{b/a} M\Delta\omega , \qquad (56)$$

where a is the scope sensitivity in volts/cm, b is the log amplifier gain in volts per decade, and M is the demagnification from scope face to film. The quantity $\Delta\omega$ is the uncertainty in signal line displacement and is therefore equal to the square root of the sum of the squares of the uncertainties in base line and signal line widths. The resulting precision in the ^{3}He and ^{4}He signals in the log region is given below.

Streak: a = 2 V/cm
b = 2.5 V/decade
M = 22.3
$\Delta\omega$ = ±4 μ
$\frac{\Delta V_i}{V_i} \approx \pm 2\%$

Raster: a = 4 V/cm
b = 2.5 V/decade
M = 22.3
$\Delta\omega$ = ±4 μ
$\frac{\Delta V_i}{V_i} \approx \pm 3\%$.

Analysis of the calibration levels in five succeeding stair-step calibrations on the streak record yields a precision of ~ ±3% in the log region, in agreement with the preceding uncertainty calculation.

For the neutron spectrum measured by the ^{3}He spectrometer, the precision is estimated to be ±5%, except for E_n > 100 keV where the ~ ±10% uncertainty in cross section dominates.

Background Problems

Figure 17 shows the Persimmon spectrum as measured by the ^{3}He(n,p)T, the ^{6}Li(n,α)T, and the ^{235}U(n,f) spectrometers (latter two combined). The deviation above E_n = 2 keV of the ^{3}He from the ^{235}U results indicates that the background provided by the ^{4}He background spectrometer is inadequate in this energy range. A glance at the ^{4}He signal at zero time in Fig. 13 or 14 reveals that the signal did not rise at the arrival of the gamma flash. The ^{4}He system was working properly, as shown by the existence of a small signal and by the normal post-data calibrations. Because the gamma flash gave rise to a large signal in the ^{3}He spectrometer but not in the identical ^{4}He spectrometer, we must look for a background mechanism dependent only on differences in nuclear properties between ^{3}He and ^{4}He. This clearly rules out such phenomena as Compton electrons produced in the windows or gas target, or electromagnetic pulse effects. The prime candidate is the nuclear photoeffect. Photodisintegration of the stable ^{4}He nucleus by (γ,n) or (γ,p) requires an energy input of ~ 19 MeV, while the ^{3}He nucleus undergoes the (γ,p) reaction at a gamma energy of 5.5 MeV. Calculations using the known fission gamma spectrum and estimating the gamma intensity from the observed neutron production show that the (γ,p) mechanism is a distinct possibility. Not much is known about the gamma spectra from inelastic scattering and other sources.

It appears that the presumed (γ,p) background generated by the gamma flash in Persimmon has invalidated the ^{3}He spectrum measurement at neutron energies above about 2 keV. Below this energy, this background appears to be negligible and not to affect the results.

11. CONCLUSION

A fast ^{3}He neutron spectrometer, free from recoil spectrum effects, has been developed and tested. Placing solid-state detectors outside the neutron beam at 90° eliminates nuclear reactions in the detectors themselves and prevents recoiling ^{3}He ions from being detected. These features are obtained at the price of a reduction in efficiency of about 10^3 compared to present ^{3}He proportional counter neutron spectrometers.

The 90° design provides an energy range up to 6 MeV, at which point it is energetically possible for the ^{3}He(n,d)D reaction to interfere. Effects of this reaction and of others at higher energies may be removed by computer calculation, and the useful energy range extended up to 10 or 20 MeV. Normal operation of the spectrometer in conjunction with a pulse-height analyzer yields the usual lower energy limit of ~ 0.1 MeV and a resolution of ~ 10%, although this can be improved by decreasing the proton acceptance angle of the solid-state detectors.

Use of the instrument in the time-of-flight current signal mode to measure the neutron spectrum in explosion source cross-section measurements offers certain advantages. The inert gaseous state of ^{3}He guarantees uniformity of target material and simplifies accurate measurement of atomic density. It appears that backgrounds peculiar to the explosion source measurements may limit the usefulness of the spectrometer to energies < ~ 2 keV in this application.

Furthermore, it seems feasible to use the ^{3}He-90° design in such applications as continuous beam monitoring or conventional time-of-flight flux monitoring.

ACKNOWLEDGMENTS

The authors acknowledge the cooperation of the members of Groups P-1, P-3, and W-8 who are directly involved in the conduct of the explosion source neutron cross-section measurements. To the many individuals, particularly in the Laboratory's Test Division, who provided invaluable support, we offer our sincere thanks.

REFERENCES

1. A. Hemmendinger et al., "Time-of-Flight Neutron Cross-Section Measurements Using Nuclear Explosions," LASL report LA-3478, Part I, 1966.
2. W. K. Brown, "A Method of Extending the Energy Range of the Helium-3 Neutron Spectrometer," Nucl. Instr. Methods 26, 1 (1964).
3. Hsien-Tsan Wang, "Inversion Matrix for a Helium-3 Fast-Neutron Spectrometer," LRL Berkeley report UCRL-10770, 1963.
4. A. Sayres and M. Coppola, "^{3}He Neutron Spectrometer Using Pulse Risetime Discrimination," Rev. Sci. Instr. 35, 431 (1964).
5. W. A. Bair, "An Improved Helium-3 Neutron Spectrometer," LRL Berkeley report UCRL-16595, 1966.
6. M. E. Lee and M. L. Awcock, "A Helium-3-filled Semiconductor Counter for the Measurement of Fast-Neutron Spectra," in Neutron Dosimetry, Proceedings of IAEA Symposium at Harwell, England, 10-14 December 1962, p. 441.
7. T. R. Jeter and M. C. Kennison, "Recent Improvements in Helium-3 Solid State Neutron Spectrometry," IEEE Trans. NS-14, 422 (1967).
8. J. Als-Nielsen, A. Bahnsen, and W. K. Brown, "Precision Measurement of Thermal Neutron Beam Densities Using a ^{3}He Proportional Counter," Nucl. Instr. Methods 50, 181 (1967); and Risø report 144, 1966.
9. J. Als-Nielsen, "Corrections in the Gold Foil Activation Method for Determination of Neutron Beam Density," Nucl. Instr. Methods 50, 191 (1967).
10. H. A. Sandmeier and G. E. Hansen, "Thermal Neutron Spectra from an Underground Nuclear Explosion with Special Consideration of Spectral Modification due to Bomb Debris Motion," LASL report LA-3403, 1965.
11. J. J. Schmidt, "Neutron Cross Sections for Fast Reactor Materials: Evaluation," report KFK-120, Part I (EANDC-E-35-U), p. A31, 1966.
12. L. Stewart, Los Alamos Scientific Laboratory, private communication.
13. R. L. Macklin and J. H. Gibbons, "On the Absolute Value and Energy Dependence of the ^{3}He(n,p)T Reaction," in The Study of Nuclear Structure with Neutrons, International Conference at Antwerp, Belgium, 19-23 July 1965 (EANDC-45-S).
14. J. E. Perry et al., "The T(p,n)He^3 Reaction and Its Inverse," as presented by J. D. Seagrave in Nuclear Forces and the Few-Nucleon Problem, Proceedings of the Conference in London, 1959 (Pergamon Press, London, 1960), p. 583.
15. M. D. Goldberg et al., "Angular Distributions of T(p,n)He^3 Neutrons for 3.4- to 12.4-MeV Protons," Phys. Rev. 122, 1510 (1961).
16. W. E. Wilson, R. L. Walter, and D. B. Fossan, "Differential Cross Sections for the T(p,n)He^3 Reaction," Nucl. Phys. 27, 421 (1961).
17. B. Antolković et al., "Study of Neutron-Induced Reactions on He^3 at E_n = 14.4 MeV," Phys. Rev. 159, 777 (1967).
18. W. Whaling, "The Energy Loss of Charged Particles in Matter," in Handbuch der Physik, Vol. 34 (Springer-Verlag, 1958), p. 193.
19. D. Demirlioglu and W. Whaling, California Institute of Technology, 1962, "Proton Stopping Cross Sections," private communication to J. McNally.
20. J. Als-Nielsen and O. Dietrich, "Slow Neutron Cross Sections for He^3, B, and Au," Phys. Rev. 133, B925 (1964).
21. W. L. Buys, "Average Energy per Pair in p-type Silicon with 5 MeV Alpha Particles," Nucl. Instr. Methods 42, 329 (1966).
22. A. Hemmendinger, M. G. Silbert, and A. Moat, "Transient Response of Solid State Detectors," IEEE Trans. NS-12, 304 (1965).
23. J. C. Bowe, "Drift Velocity of Electrons in Nitrogen, Helium, Neon, Argon, Krypton, and

Xenon," Phys. Rev. 117, 1411 (1960).

24. W. P. Jesse and J. Sadauskis, "Ionization in Pure Gases and the Average Energy to Make an Ion Pair for Alpha and Beta Particles," Phys. Rev. 97, 1668 (1955).

25. A. L. Morse et al., "Far Ultraviolet Response of Silicon P-N Junction Photodiodes," USC report USC Vac UV-101, 1965.

26. J. S. Lunsford, "Logarithmic Pulse Amplifier," Rev. Sci. Instr. 36, 461 (1965).

27. P. A. Seeger and D. W. Bergen, "Time-of-Flight Neutron Cross Section Measurements Using Nuclear Explosions," LASL report LA-3478, Part II, 1966.

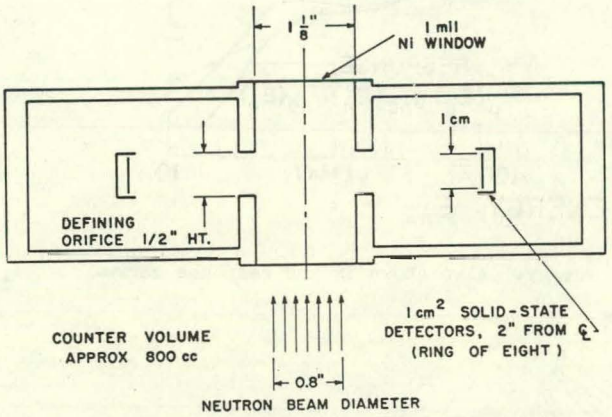

Fig. 1. Helium-3 spectrometer cross section.

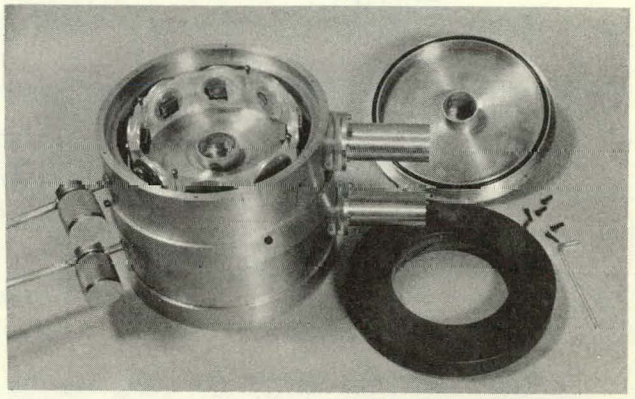

Fig. 2. Helium-3 spectrometer with top removed.

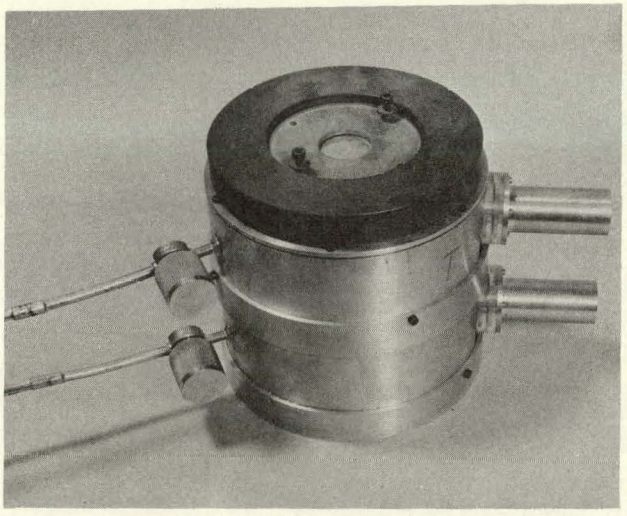

Fig. 3. Helium-3 and helium-4 spectrometers assembled.

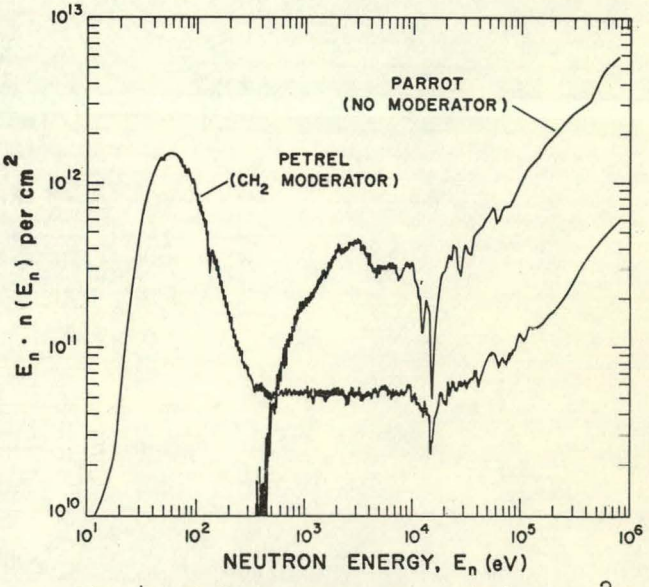

Fig. 4. Neutron spectra, $E_n \cdot n(E_n)$ per cm^2 vs E_n, for the Parrot and Petrel experiments. (Collimator orifices: Parrot, 1.037 cm^2; Petrel, 2.85 cm^2.)

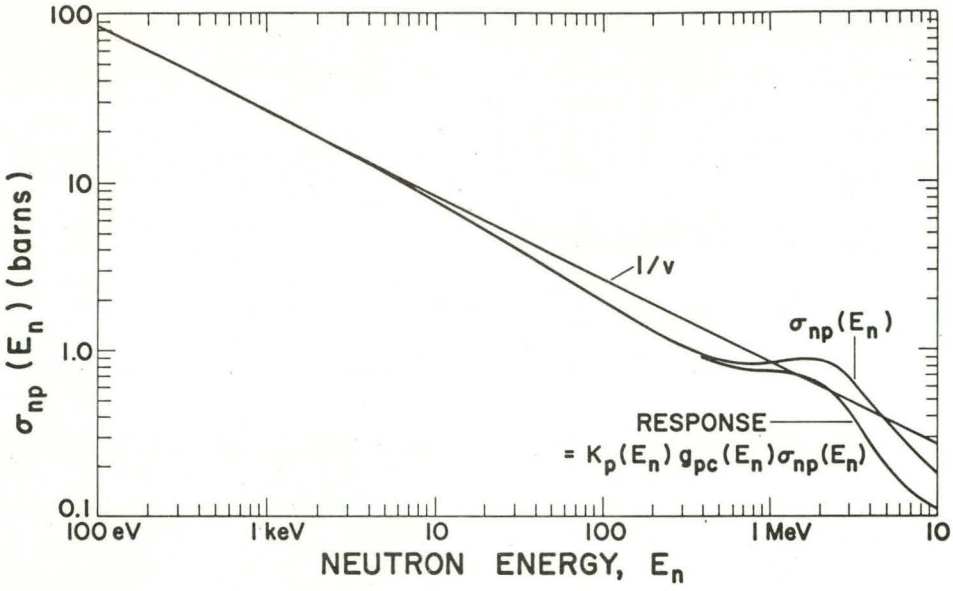

Fig. 5. ^{3}He(n,p)T cross section vs neutron energy. Also shown is the response curve.

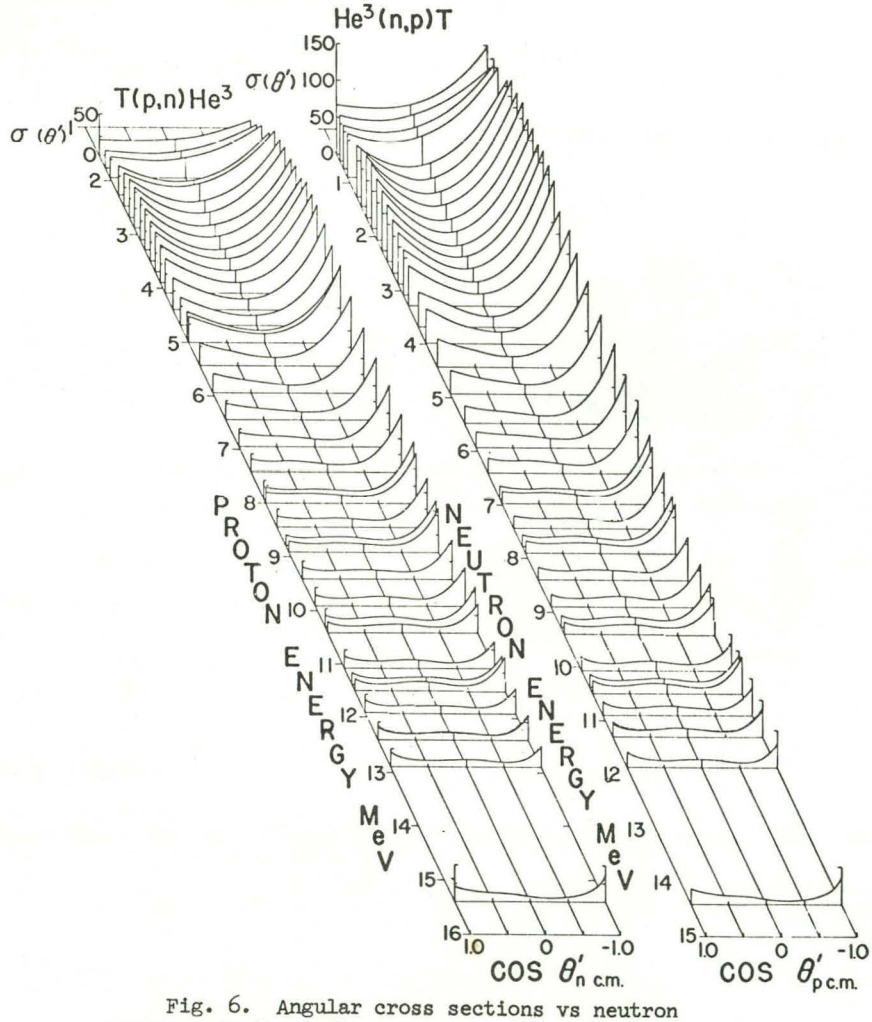

Fig. 6. Angular cross sections vs neutron energy. On the left, curves have been fitted to the measured values of the T(p,n)^{3}He reaction. The ^{3}He(n,p)T curves on the right were obtained by detailed balance from the T(p,n)^{3}He curves.

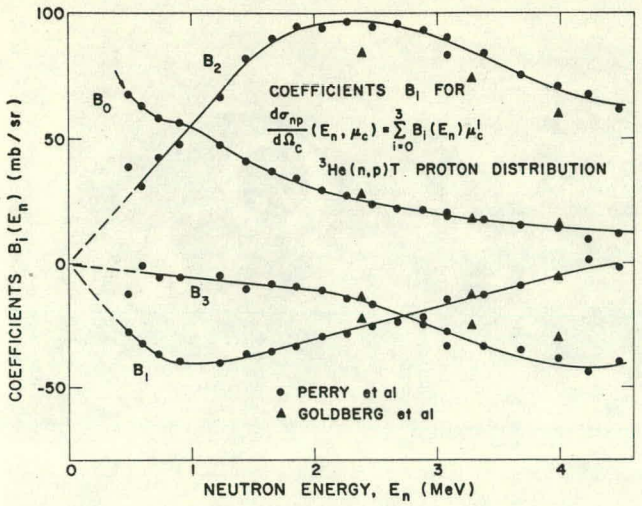

Fig. 7. Coefficients of the cosine series describing the angular proton distribution of the ^{3}He(n,p)T reaction vs neutron energy. Individual points were obtained by detailed balance from the coefficients of the cosine series fits to the inverse reaction T(p,n)^{3}He. Low energy values were estimated by extrapolation of the curves back to zero energy (dotted lines).

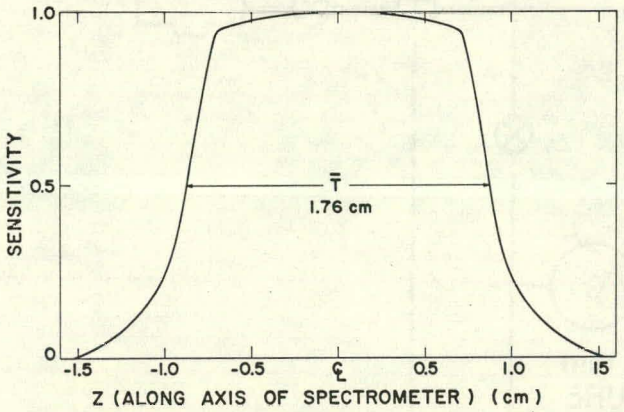

Fig. 9. Sensitivity as a function of location along the axis of the counter, normalized to unity at the centerline.

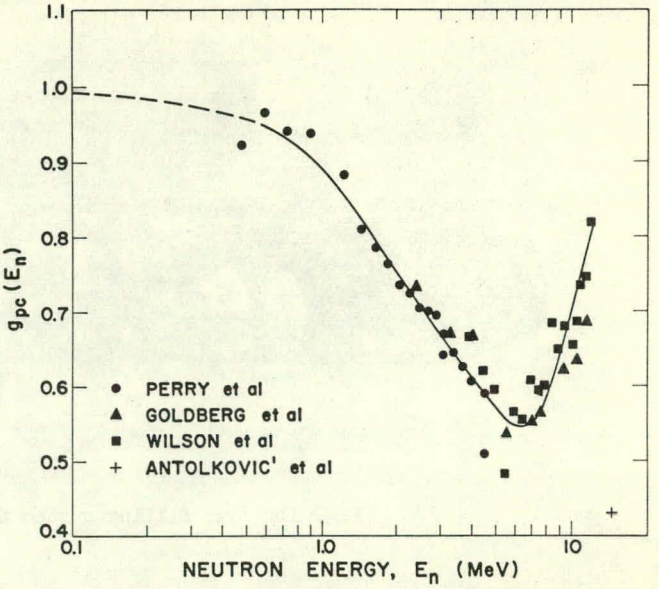

Fig. 8. The function $g_{pC}(E_n)$ vs E_n describing the relative probability of a proton from the ^{3}He(n,p)T reaction being emitted at the particular angle in the C system corresponding to 90° in the L system. The values at low energies (dotted lines) were calculated from the extrapolated cosine coefficients.

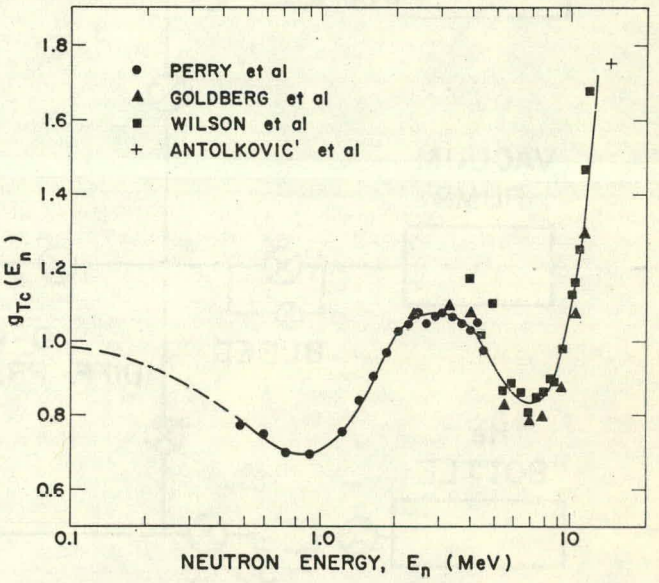

Fig. 10. The function $g_{TC}(E_n)$ vs E_n describing the relative probability of a triton from the ^{3}He(n,p)T reaction being emitted at the particular angle in the C system corresponding to 90° in the L system.

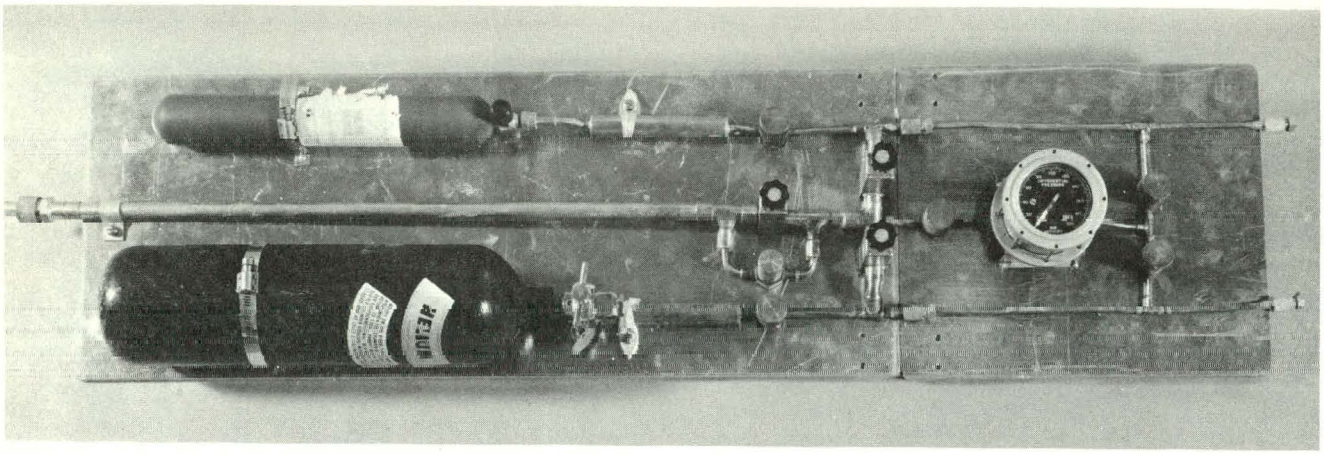

Fig. 11. Gas filling system for the ^{3}He and ^{4}He spectrometers.

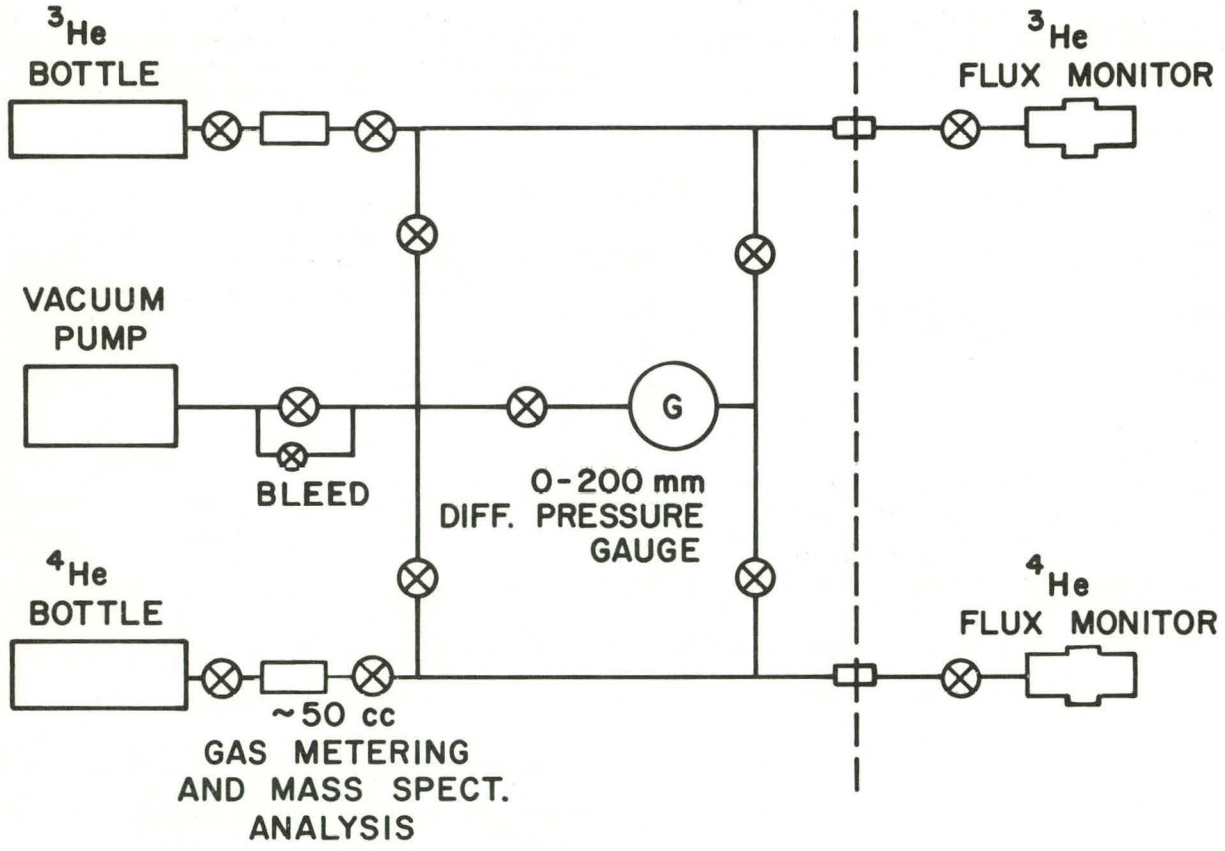

Fig. 12. Gas filling system schematic for the ^{3}He and ^{4}He spectrometers.

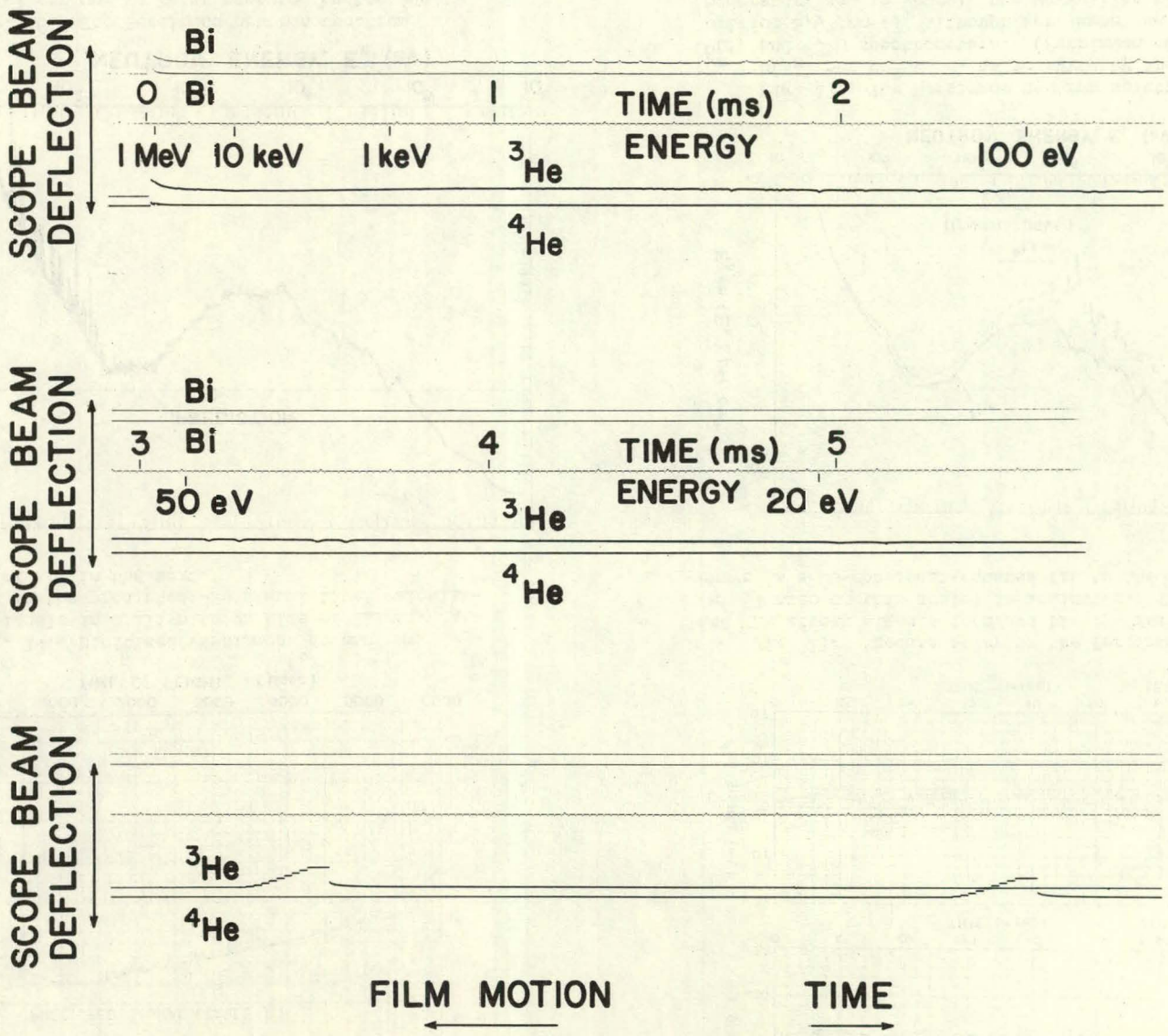

Fig. 13. The ^{3}He and ^{4}He streak signals from the Persimmon experiment. Timing signals and postdata calibrations are shown.

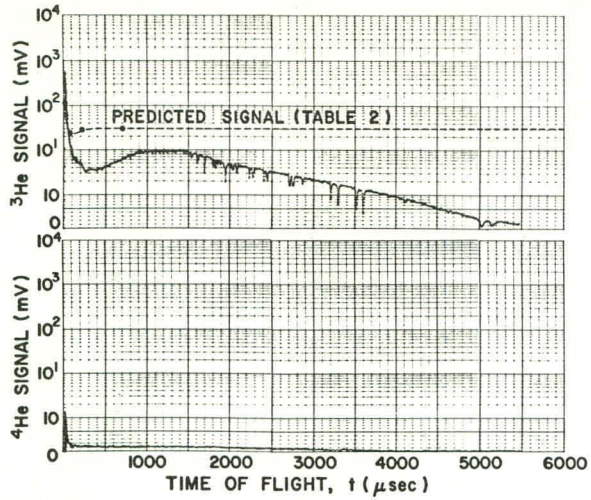

Fig. 14. Digitized Persimmon ^{3}He and ^{4}He streak signals in millivolts vs time of flight. Also shown is the predicted ^{3}He signal level calculated in Table II in the text.

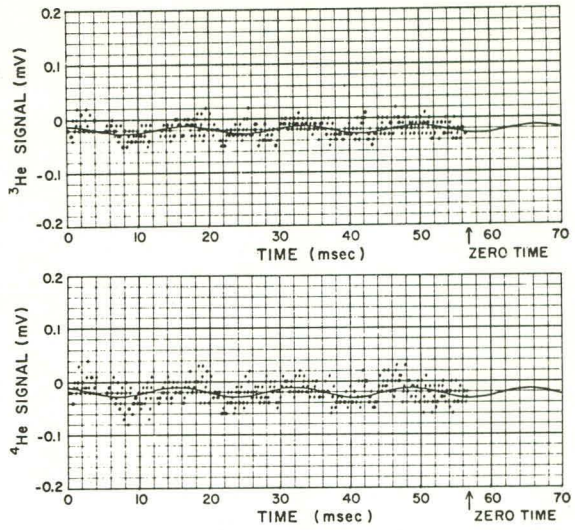

Fig. 15. Predata noise on the Persimmon ^{3}He and ^{4}He streak signals in mV vs time. "Zero time" (at 57 msec on this scale) is indicated. The solid curve is a 60-cps least-squares fit to the points.

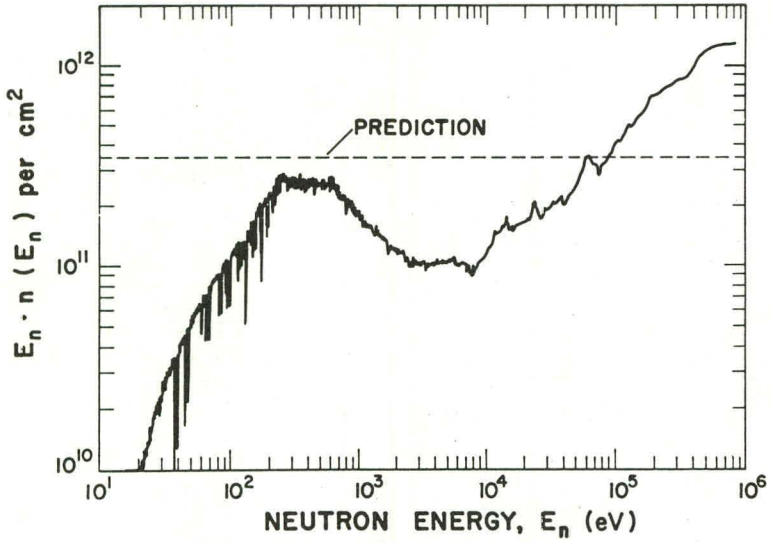

Fig. 16. The Persimmon neutron spectrum $E_n \cdot n(E_n)$ per cm^2 vs E_n as measured by the ^{3}He, ^{4}He spectrometer pair. (Persimmon collimator orifice 2.97 cm^2.)

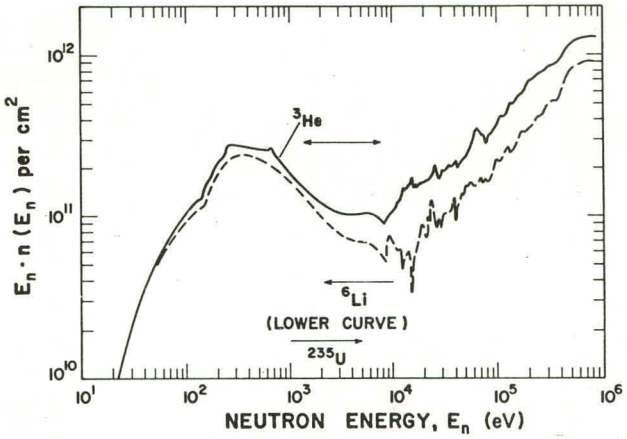

Fig. 17. The Persimmon neutron spectrum $E_n \cdot n(E_n)$ per cm^2 vs E_n as measured by the ^{3}He, ^{6}Li, and ^{235}U spectrometers. (Persimmon collimator orifice 2.97 cm^2.) Although Persimmon had a CH_2 moderator, as did Petrel, the Maxwellian thermal peak is missing owing to earlier closure of the vacuum pipe.